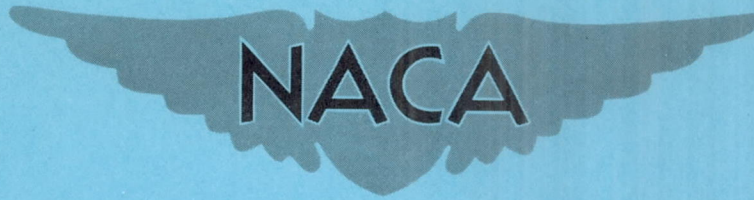


NACA RM A57G10

RM A57G10



# RESEARCH MEMORANDUM

FLIGHT INVESTIGATION OF THE LOW-SPEED CHARACTERISTICS  
OF A 35° SWEPT-WING AIRPLANE EQUIPPED WITH AN AREA-  
SUCTION EJECTOR FLAP AND VARIOUS WING LEADING-  
EDGE DEVICES

By Seth B. Anderson, Alan E. Faye, Jr.,  
and Robert C. Innis

Ames Aeronautical Laboratory  
Moffett Field, Calif.

**NATIONAL ADVISORY COMMITTEE  
FOR AERONAUTICS  
WASHINGTON**

September 26, 1957  
Declassified September 17, 1958

NATIONAL ADVISORY COMMITTEE FOR AERONAUTICS

RESEARCH MEMORANDUM

FLIGHT INVESTIGATION OF THE LOW-SPEED CHARACTERISTICS  
OF A 35° SWEEP-WING AIRPLANE EQUIPPED WITH AN AREA-  
SUCTION EJECTOR FLAP AND VARIOUS WING LEADING-  
EDGE DEVICES

By Seth B. Anderson, Alan E. Faye, Jr.,  
and Robert C. Innis

SUMMARY

Tests have been conducted to determine the flight characteristics of an F-86F airplane equipped with an area-suction-type boundary-layer control installation on the trailing-edge flaps. Ejector pumps enclosed within the flaps were used for suction. Flap lift increments were determined in conjunction either with a slatted leading edge or with an inflatable rubber boot on the wing leading edge. Measurements were made of the lift, drag, and engine bleed-air requirements. The results of the flight tests are compared with those of flight tests of a blowing-flap-type boundary-layer control system on the same airplane.

The most interesting part of the results was considered to be the effect that the wing leading edge had on the magnitude of the flap lift increment, particularly at maximum lift coefficient. The flap lift increment was increased from 0.39 to 0.50 at maximum lift coefficient by changing from the slatted leading edge to the inflatable rubber boot leading edge.

In the comparison of the relative performance of suction and blowing based on the use of an equal amount of engine bleed air, it was found that a blowing flap produced approximately twice the value of increased lift due to boundary-layer control as did the area-suction ejector flap in the angle-of-attack range for landing approach.

## INTRODUCTION

The NACA has completed a number of flight investigations of the use of boundary-layer control to improve the low-speed characteristics of high-speed airplanes (refs. 1 through 4). These flight tests have shown a general improvement in low-speed characteristics due to boundary-layer control. A problem in providing suction boundary-layer control is that of finding a practical pumping system. One means of pumping recently tested was an area-suction type trailing-edge flap with a number of ejector pumps enclosed within the flap itself. The ejector flap was tested on a swept-wing carrier-type aircraft (ref. 4) in which the ejectors were designed to be most efficient in the engine power range used for carrier approach.

A similar type ejector flap was developed under contract for the Air Force; however, it was designed to be most efficient at low engine speeds used in a sinking-type (Air Force type) landing approach. This was accomplished by using enlarged pump nozzles to provide increased pumping capabilities even though the engine is run at low speeds. This flap included a geared, split flap on the lower surface of the main flap for the purpose of improving the ejector pumping characteristics and to close off the ejector exits when the main flap was in the up position.

At the request of the Air Force, Wright Air Development Center, (WADC), this flap was tested on an F-86F airplane at the Ames Aeronautical Laboratory. The flap was tested in conjunction with a slatted leading edge and an inflatable rubber boot on a fixed leading edge. In some cases the results of the flight tests are compared with results obtained using a blowing flap (ref. 3) tested on the same airplane.

## NOTATION

b	wing span
BLC	boundary-layer control
$C_D$	drag coefficient, $\frac{\text{drag}}{qS}$
$C_L$	lift coefficient, $\frac{\text{lift}}{qS}$
$\Delta C_L$	increment in lift coefficient due to flaps
$C_{L_{\text{max}}}$	maximum lift coefficient

$\bar{c}$	local wing chord, ft
L.E.	leading edge
$p$	free-stream static pressure, lb/sq ft
$p_d$	total pressure in flap duct, lb/sq ft
$P_f$	duct pressure coefficient, $\frac{p_d - p}{q}$
$q$	dynamic pressure, lb/sq ft
$S$	wing area, sq ft
$w$	engine bleed-air flow, lb/sec
$\alpha$	angle of attack, deg

#### EQUIPMENT AND TESTS

The installation of the area-suction ejector flap was made on an F-86F airplane. A drawing of the airplane is presented in figure 1. Pertinent dimensions of the airplane are given in table I. A general view of the airplane and a close-up of the flap are presented in figures 2 and 3, respectively. The suction system consisted of a manifold to collect air from the last stage of the compressor of the J47-GE-27 engine, a valve controlled by the pilot, and ducting on the underside of the fuselage to each flap.

The flap was a plain type with the same geometry as the types tested in references 1 and 3 except that the inboard flap end was shaped to be streamwise when the flap was deflected  $55^\circ$ . The flap was designed and constructed for the F-86F airplane by Research, Inc., Minneapolis, Minnesota, under contract from WADC. A sketch of the flap cross section is presented in figure 4. Each flap contained 11 double-nozzle ejector pumps. Photographs showing the undersurface of the flap and the ducting at the root of the flap are presented in figures 5 and 6, respectively. In the initial testing, a split flap was used on the lower surface of the main flaps (see fig. 7). The split flap had a gearing ratio of 1.4:1 with respect to the main surface, and was adjusted to close off the ejector exits when the main flap was undeflected. Air entered the root of the flap by means of an O-ring rotating seal located on an axis above the flap hinge line. In order to take care of translation of the ducting at the seal, a rubber tube was used inside a telescoping metal shield as shown in figure 6. This ducting installation provided a "cleaner" aerodynamic design at the flap-fuselage juncture than that which existed for

the tests in reference 1 since it was found in the tests of reference 1 that conditions at the flap-fuselage juncture influenced the flap lift appreciably. It was not feasible to make the ducting installation internal because of interference with fuel tanks.

Boundary-layer air was removed from the upper surface above the hinge line of the flap through two types of porous material. One type was sintered stainless steel similar to that tested in reference 1. Another was a porous surface consisting of perforated 2024-T3 aluminum (fig. 8) having a hole spacing pattern designed to give pressure drop characteristics and velocity characteristics equal to those for the sintered stainless steel of reference 1. A more complete description of various types of porous surfaces is given in reference 5. The majority of results presented herein are for the perforated material.

Tests were conducted with two types of wing leading-edge devices. One of these was the 6-3 slat which is described in reference 3; the other an inflatable rubber boot bonded to a solid 6-3 leading edge also described in reference 3. The boot was developed by the B. F. Goodrich Company under contract from WADC. The airfoil sections were similar to those described in reference 3. The end of the boot tested herein extended 10 inches farther inboard than the boot tested in reference 3. Sketches of the boot profile at two spanwise stations and for two values of internal pressure are shown in figure 9.

Standard NACA instruments were used to record airspeed, altitude, acceleration, duct pressures, and angle of attack. Values of airspeed and angle of attack were measured approximately 8 feet ahead of the fuselage nose. Duct pressures in the flap were measured at the midspan station of the flap. Measurements with a flow meter indicated uniform inflow velocities through the porous material along the span of the flap at zero forward velocity.

Tests were conducted at an average altitude of 5,000 feet in steady straight flight over a speed range from 160 knots to the stall. The average wing loading was 46 pounds per square foot and the center of gravity was located at 0.26 mean aerodynamic chord.

## RESULTS

The test results of this investigation are presented in figures 10 through 14. For the most part the results presented herein with the area-suction ejector flap are similar to those obtained with the other boundary-layer control flap systems tested (refs. 1, 3, and 4). In this regard improvements in flap lift due to BLC were obtained over the operational speed range of the airplane. The discussion in this report is limited to those points considered of major interest.

Early in the flight tests it was found that an appreciable reduction in flap lift ( $\Delta C_L = 0.05$ ) occurred over the entire angle of attack range when the split flap was deflected from the main flap. The results presented herein are those for the test condition with the split flap removed.

There were no appreciable differences in the aerodynamic results between the sintered stainless steel surface and the perforated aluminum surface used on the suction area of the flaps. This is of interest in view of the relatively large holes and spacing pattern used in the perforated material (for a more complete discussion of perforated materials, see ref. 6). It was felt, however, from an operational, service standpoint, that the perforated material would be superior because of less tendency for clogging; however, during the course of flight testing at this laboratory no clogging of porous material was measured.

## DISCUSSION

### Aerodynamic Characteristics

Effect of leading edge.- For most wing configurations reported (refs. 1, 3, and 4) it has been found generally that when boundary-layer control was applied to a trailing-edge flap,  $C_{L_{max}}$  was reached at a lower angle of attack and the flap lift increment was reduced in the  $\alpha$  range near  $C_{L_{max}}$ . This is exemplified in the data in figures 10(a) and 11 for the configuration with the 6-3 slatted leading edge. It has been demonstrated that the foregoing lift characteristic is typically a result of flow separation from the wing leading edge which is induced by the added circulation around the wing due to the application of boundary-layer control to the trailing-edge flap. With increased leading-edge stall protection, improvements in maximum lift and flap lift increment can be realized at higher values of angle of attack. Such leading-edge protection is illustrated in the data of figure 10(b) which show that with the inflatable rubber boot, maximum lift with boundary-layer control on occurred at  $3^\circ$  higher angle of attack compared to the boundary-layer control off condition. In addition to the improvement in  $C_{L_{max}}$  it can be noted (fig. 11) that the flap lift increment was increased over that obtained with the slatted leading edge and showed essentially no deterioration with increase in angle of attack. The reason for the marked increase in  $\alpha$  for maximum lift which occurred with boundary-layer control on is not known; in fact this phenomenon was not obtained on all flights (e.g., see fig. 10(c)). In addition this type of lift increase was not obtained with the cambered leading edge tested in reference 1 or the inflatable rubber boot tested in reference 3.

An attempt was made to pin down the inconsistencies in maximum lift by leading-edge configuration changes. One change readily made with the inflatable boot was a change in leading-edge radius obtained by increasing internal pressure from 10 to 20 pounds per square inch gage. As can be observed from a comparison of the data in figures 10(c) and 10(d), the increase in leading-edge radius did not result in a change in maximum lift. This indicates that small changes in leading-edge radius which might occur due to fluctuations in internal boot pressures were not responsible for the large variations in maximum lift previously noted. Studies of tuft behavior on the upper wing surface showed distinctly different stall patterns associated with the changes in maximum lift presented in figures 10(b) and 10(c). When the higher value of maximum lift was obtained, air flow separation occurred initially at the wing trailing edge (on the ailerons) spreading forward slowly with increase in angle of attack. When the lower value of maximum lift was obtained, a leading-edge type separation took place initially at the wing tips and progressed inboard rapidly with increase in  $\alpha$ . The foregoing illustrates a condition where stalling is imminent from either the wing leading or trailing edges. Although it is not known what flight conditions are necessary to cause one type of stall to take precedence, it appears that when trailing-edge separation occurred first, the tendency for leading-edge separation was delayed with a resultant over-all increase in  $C_{L_{max}}$ .

Effect of engine rpm on lift.- For the data presented herein, the bleed-air control valve was in the full open position for all engine speeds; consequently the suction pressures, exhaust air momentum, and therefore flap lift increment, were a function of engine speed. The variation of flap lift increment with engine speed is presented in figure 12. Included in this figure for comparison purposes are data from the blowing flap of reference 3 corrected to correspond to the same amount of engine bleed air as used by the ejector flap. These results show that greater values of lift were obtained with the blowing-flap system over the complete rpm range. At an engine speed for landing approach (80 percent) use of the blowing-flap system resulted in over twice the increase in lift measured from the boundary-layer control off condition as compared to the suction system. In general, each type system showed similar variation in lift with engine speed.

Effect of BLC and type of wing leading edge on drag.- Drag data in figure 10 indicate an increase in drag with suction on at all except the highest lift coefficient values. These results are similar to others (refs. 1 and 3) with boundary-layer control applied to a partial-span flap. It can be noted that, in general, the drag for a given  $C_L$  was smaller with the inflatable boot than with the slatted leading edge (see figs. 10(a) and 10(b)).

Effect of flap deflection.- The flap lift increments obtained at various flap deflections are presented in figure 13 for an angle of attack

of  $8^\circ$ . Included in this figure are data obtained from the blowing-flap tests of reference 3. The theoretical flap lift increments were calculated by the method of reference 7. The results for the ejector flap with boundary-layer control on and  $55^\circ$  flap deflection show values of flap lift increment approximately 70 percent of theoretical while the values obtained with the blowing flap were slightly greater than those predicted by theory. For the ejector flap only small increases ( $\Delta C_L = 0.02$ ) in flap lift increment were obtained when the flap deflection was increased from  $45^\circ$  to  $66^\circ$ .

#### Miscellaneous Characteristics

Pumping.- The arrangement of the pumping equipment in the flap precluded the measurement of suction flow quantities directly. It was possible, however, to indicate whether adequate flow and pumping pressures were available. This was done by measuring the flap duct pressures and noting the variation of flap lift with duct pressure. An examination of the data in figure 14 shows that at a  $P_f$  of -2 the knee of the curve (indicating flow attachment) was reached and much larger pressure coefficients were available. The continued rise in lift at these larger pressure coefficients is felt to result from increased circulation around the flap induced by the jet exhaust from the lower surface of the flap. It is noteworthy that no similar increase in lift was obtained when the air was exhausted underneath the fuselage for the pumping system used in reference 1.

Stalling characteristics.- Boundary-layer control produced essentially no difference in stalling behavior for either of the leading edges tested. With the slatted leading edge, flap deflected  $55^\circ$ , the stall was considered marginally satisfactory chiefly because of the presence of a pitch-up which was considered mild. There was no aerodynamic stall warning. With the inflatable leading edge, boot deflated, the stall behavior was characterized by a slow right roll-off, the stall being considered unsatisfactory because of inability to stop rolling before an angle of bank of  $45^\circ$  was reached. The stall warning was satisfactory. With the boot inflated the roll-off was more abrupt; there was no stall warning.

On one occasion when the boot was being deflated in flight, ridges formed in the rubber near the leading edge. This resulted in a leading-edge stall at a relatively high airspeed (160 knots), a condition which was extremely disconcerting to the pilot. This difficulty could have been overcome by coating the inner surface of the rubber with an oil-graphite mixture.

Trim changes.- The trim changes due to application of boundary-layer control were considered small.



## SUMMARY OF RESULTS

The following results are based on measurements of the flight characteristics of an F-86F airplane equipped with area-suction-type boundary-layer control on the trailing-edge flap:

1. The type of wing leading edge used had a marked effect on the magnitude of the flap lift increment in the angle-of-attack range near maximum lift. With boundary-layer control on the flap, an increase in flap lift increment from 0.39 to 0.50 was obtained in changing from a slatted leading edge to an inflatable rubber boot leading edge.

2. The area-suction flap achieved flap lift values 70 percent of that theoretically obtainable at a flap deflection of  $55^\circ$  and angle of attack of  $8^\circ$  whereas a blowing flap tested on the same airplane achieved flap lift values slightly greater than theoretical.

3. The increase in lift (at a constant angle of attack) due to the application of BLC was twice as great for the blowing flap as for the area-suction flap compared on the basis of using equal amounts of engine bleed air.

4. There were no appreciable differences in aerodynamic characteristics obtained in tests for which the porous material was sintered stainless steel or perforated aluminum sheet.

5. Stalling behavior was unchanged with the use of boundary-layer control for either wing leading edge tested.

6. The longitudinal trim changes due to application of boundary-layer control were considered small.

Ames Aeronautical Laboratory  
National Advisory Committee for Aeronautics  
Moffett Field, Calif., July 10, 1957.

## REFERENCES

1. Anderson, Seth B., and Quigley, Hervey C.: Flight Measurements of the Low-Speed Characteristics of a  $35^\circ$  Swept-Wing Airplane With Area-Suction Boundary-Layer Control on the Flaps. NACA RM A55K29, 1956.
2. Bray, Richard S., and Innis, Robert C.: Flight Tests of Leading-Edge Area Suction on a Fighter-Type Airplane With a  $35^\circ$  Sweptback Wing. NACA RM A55C07, 1955.

3. Anderson, Seth B., Quigley, Hervey C., and Innis, Robert C.: Flight Measurements of the Low-Speed Characteristics of a  $35^{\circ}$  Swept-Wing Airplane With Blowing-Type Boundary-Layer Control on the Trailing-Edge Flaps. NACA RM A56G30, 1956.
4. Quigley, Hervey C., Hom, Francis W. K., and Innis, Robert C.: A Flight Investigation of Area-Suction and Blowing Boundary-Layer Control on the Trailing-Edge Flaps of a  $35^{\circ}$  Swept-Wing Carrier-Type Airplane. NACA RM A57B14, 1957.
5. Dannenberg, Robert E., Gambucci, Bruno J., and Weiberg, James A.: Perforated Sheets as a Porous Material for Distributed Suction and Injection. NACA TN 3669, 1956.
6. Dannenberg, Robert E., Weiberg, James A., and Gambucci, Bruno J.: Perforated Sheets as the Porous Material for a Suction-Flap Application. NACA TN 4038, 1957.
7. DeYoung, John: Theoretical Symmetric Span Loading Due to Flap Deflection for Wings of Arbitrary Plan Form at Subsonic Speeds. NACA Rep. 1071, 1952.

TABLE I.- DIMENSIONS OF TEST AIRPLANE

Wing	
Total area, sq ft . . . . .	302
Span, ft . . . . .	37.12
Aspect ratio . . . . .	4.79
Taper ratio . . . . .	0.51
Mean aerodynamic chord (wing station 98.7 in.), ft . . . . .	8.1
Dihedral angle, deg . . . . .	3.0
Sweepback of 0.25-chord line, deg . . . . .	35.23
Geometric twist, deg . . . . .	2.0
Root airfoil section (normal to 0.25-chord line) . . . . .	NACA 0012-64 (modified)
Tip airfoil section (normal to 0.25-chord line) . . . . .	NACA 0011-64 (modified)
Wing area affected by flap, sq ft . . . . .	116.6
Horizontal tail	
Total area, sq ft . . . . .	35.0
Span, ft . . . . .	12.7
Aspect ratio . . . . .	4.65
Taper ratio . . . . .	0.45
Dihedral angle, deg . . . . .	10.0
Mean aerodynamic chord (horizontal-tail station 33.54 in.), ft . . . . .	2.9
Sweepback of 0.25-chord line, deg . . . . .	34.58
Airfoil section (parallel to center line) . . . . .	NACA 0010-64
Vertical tail	
Total area, sq ft . . . . .	34.4
Span, ft . . . . .	7.5
Aspect ratio . . . . .	1.74
Taper ratio . . . . .	0.36
Sweepback of 0.25-chord line, deg . . . . .	35.00
Flap	
Total area, sq ft . . . . .	23.7
Span (from 13.4 to 49.5-percent semispan), ft . . . . .	7.27
Chord (constant), ft . . . . .	1.67

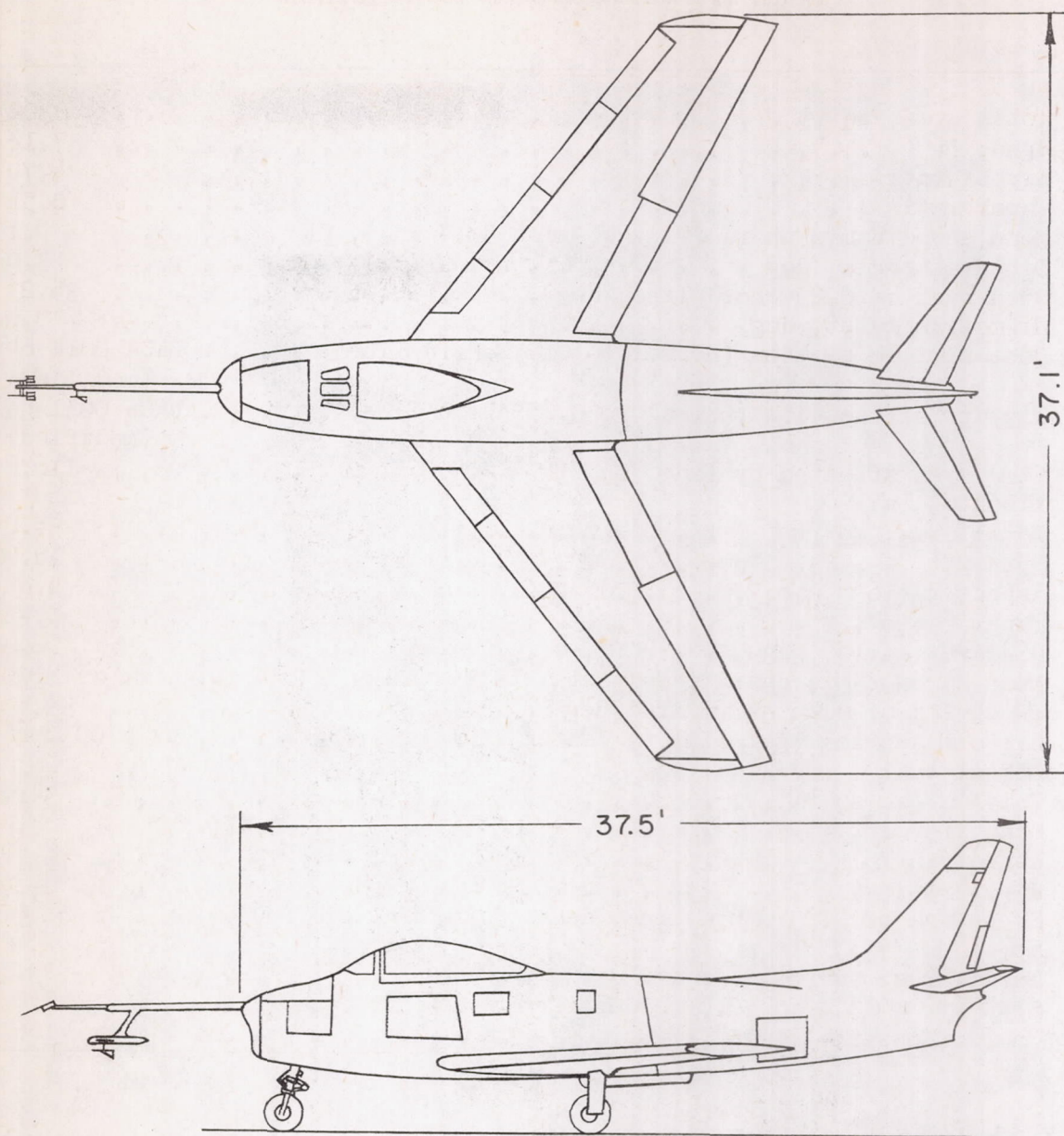
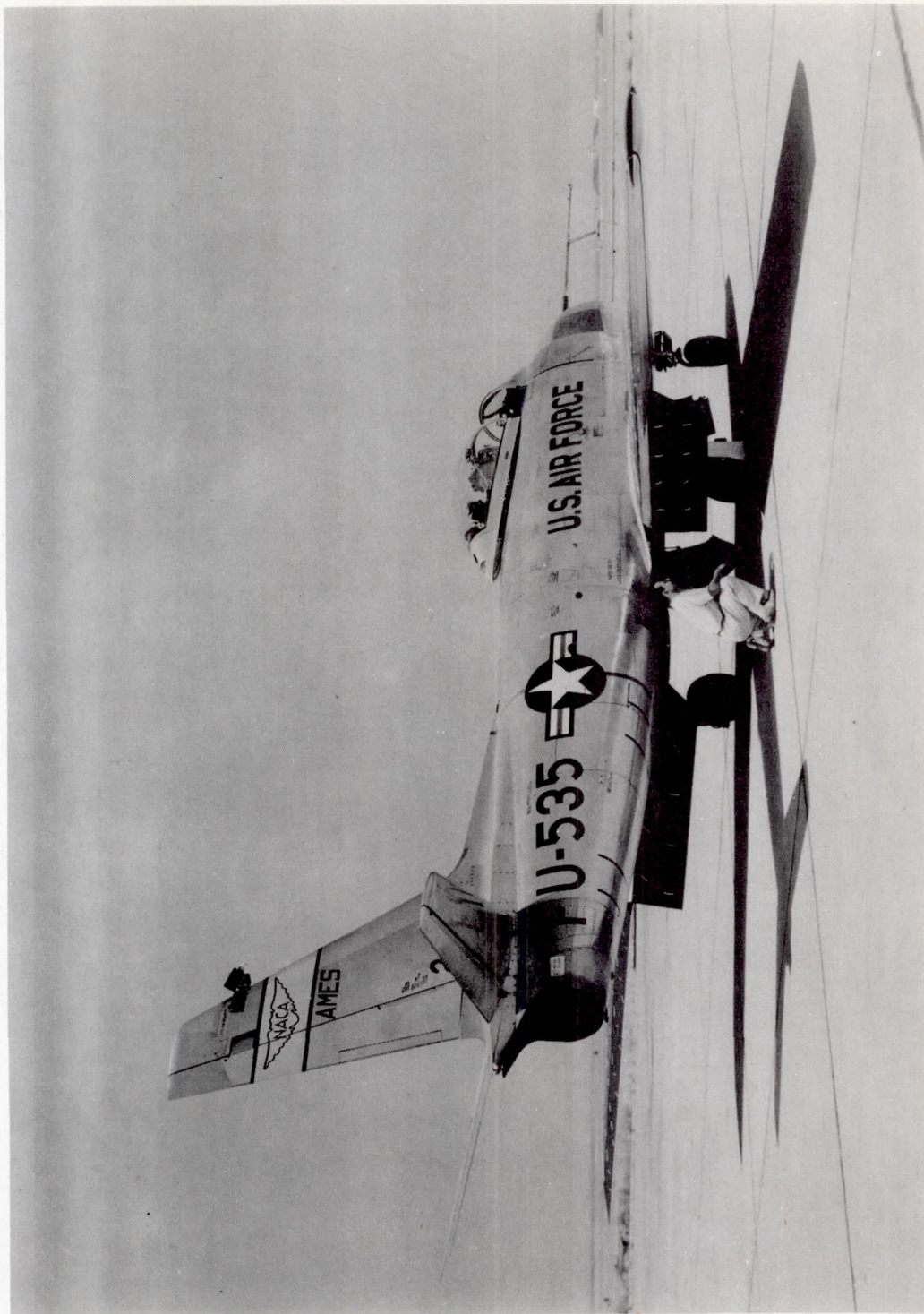
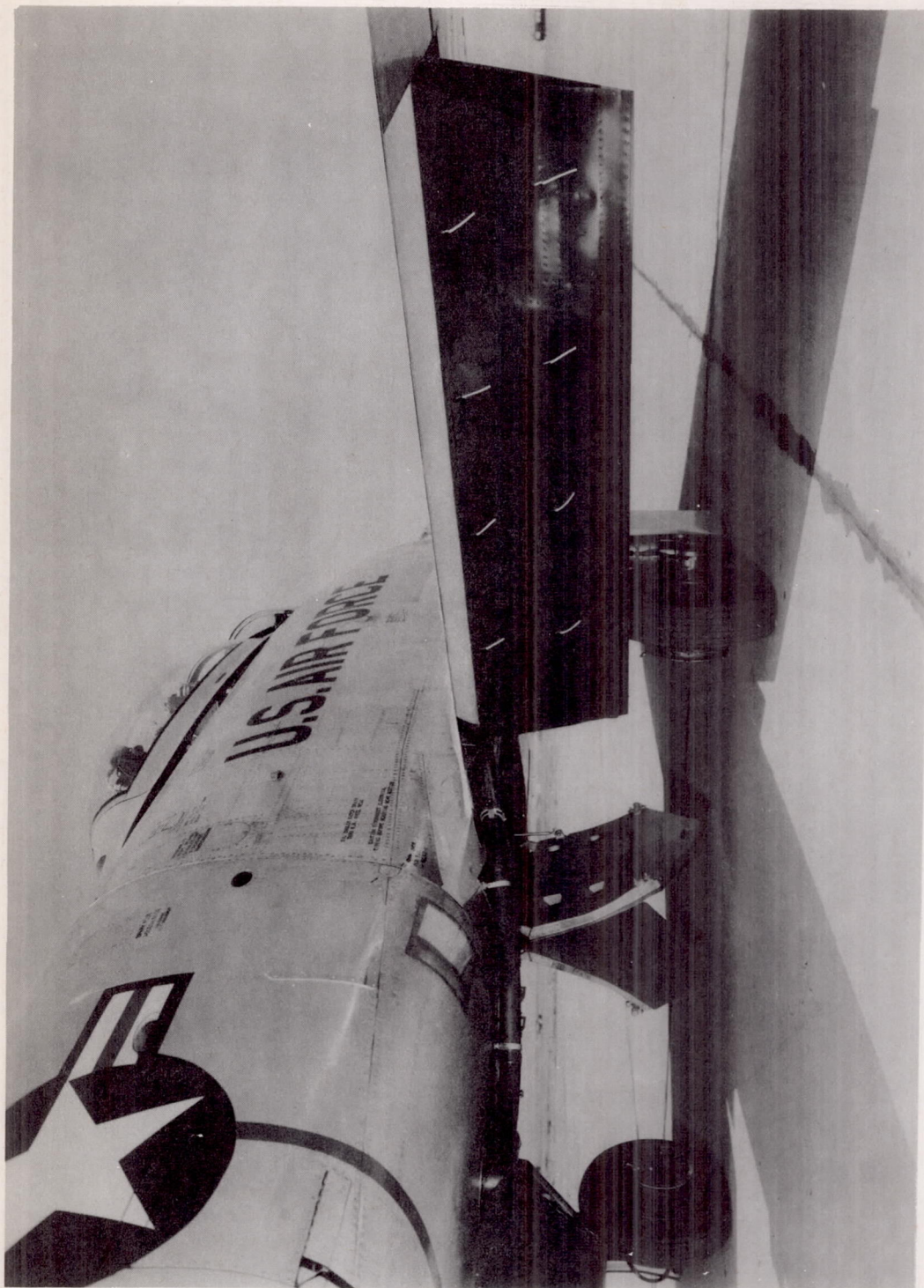


Figure 1.- Drawing of test airplane.



A-21685

Figure 2.- View of test airplane.



A-21686

Figure 3.- Close-up of flap.

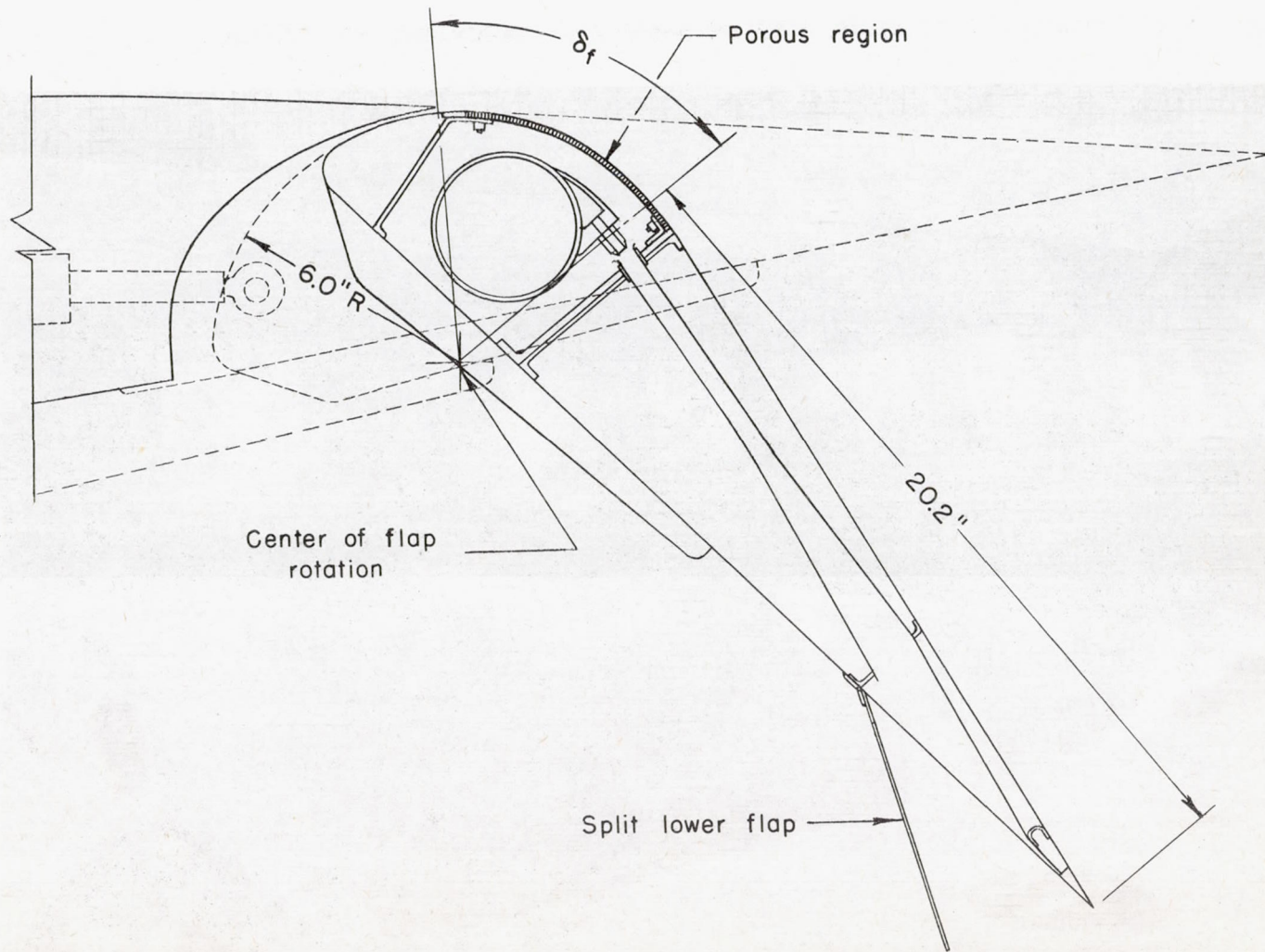


Figure 4.- Cross section of ejector flap.

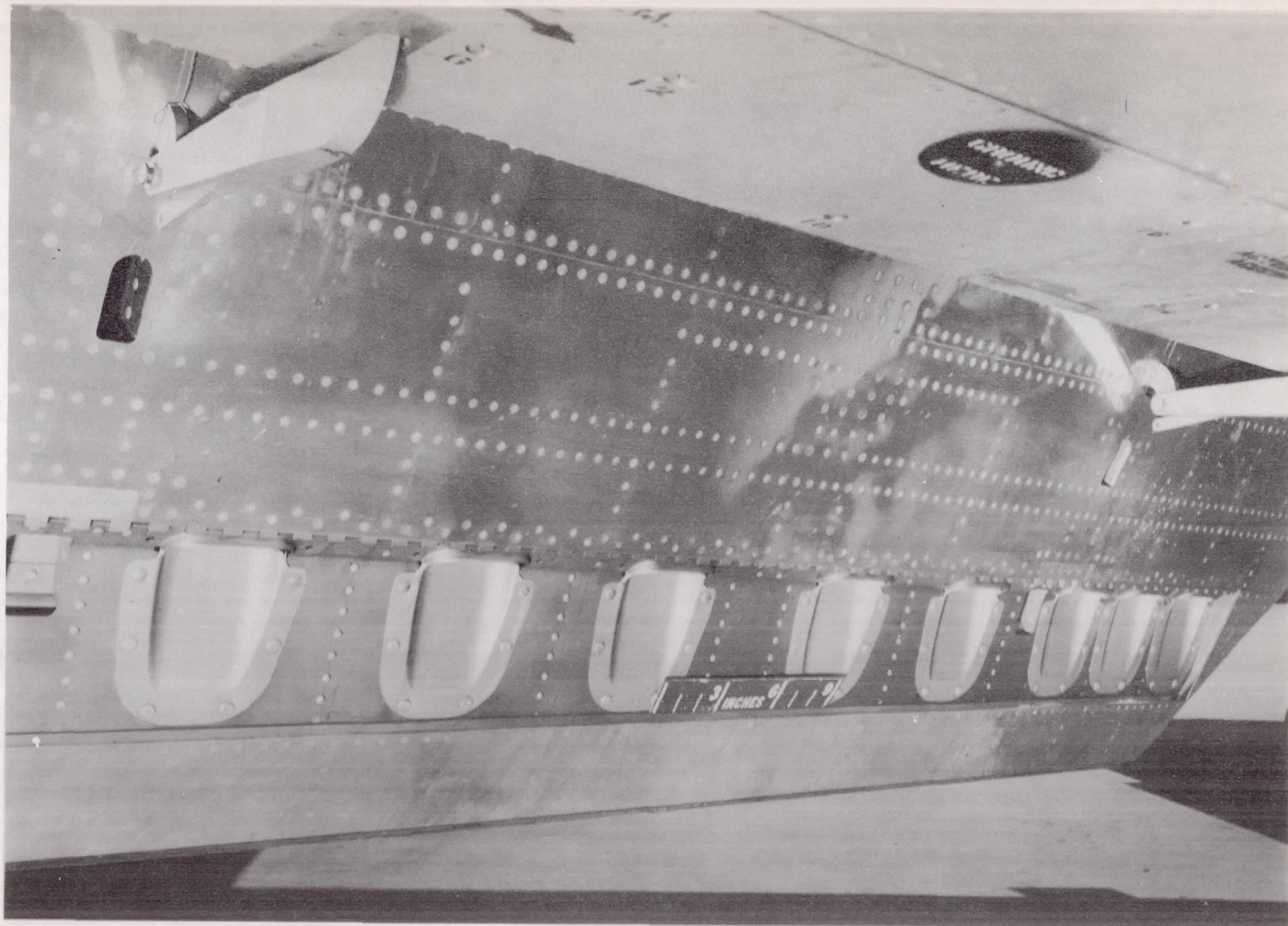


Figure 5.- Undersurface of ejector flap; split flap removed.

A21687



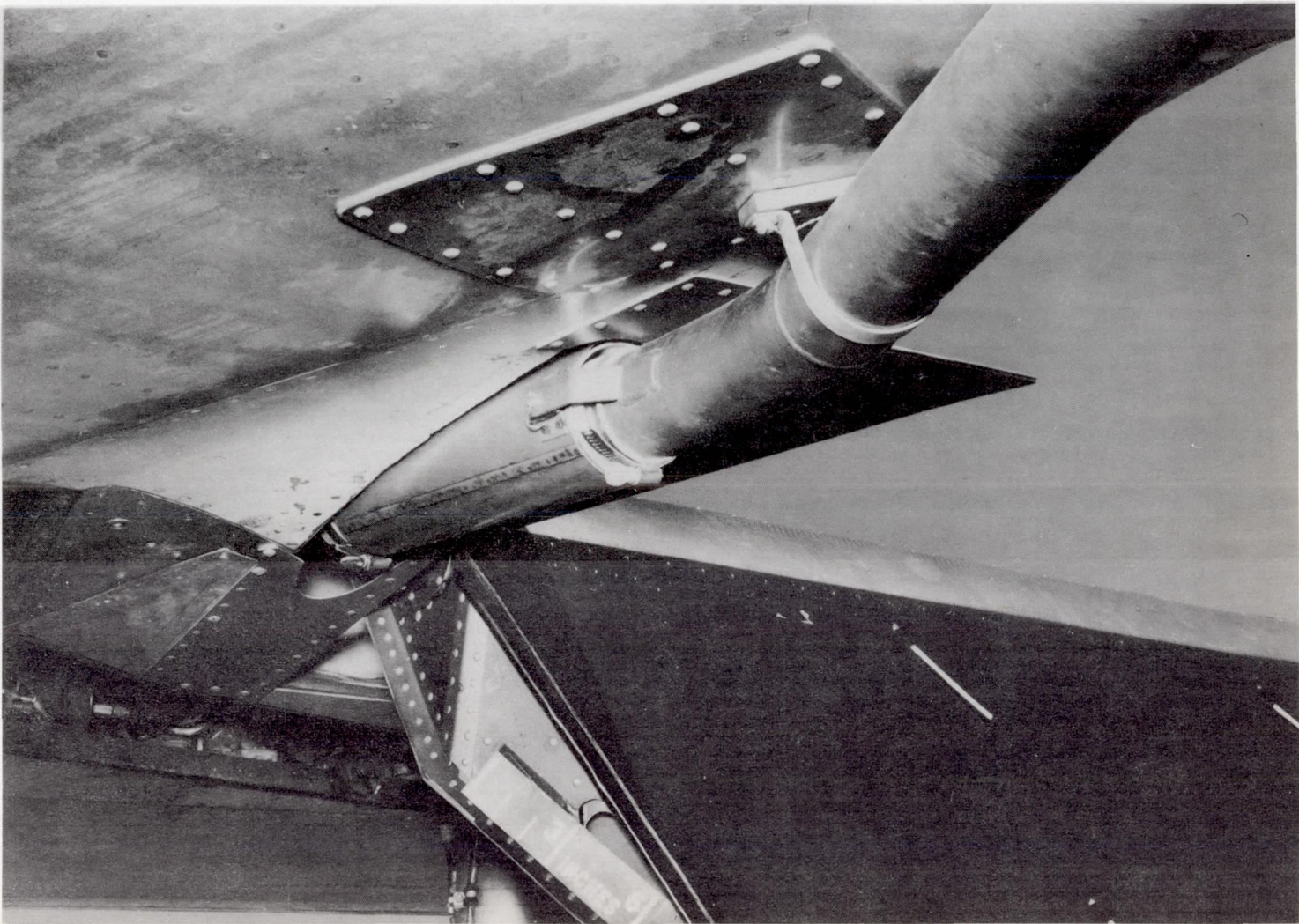
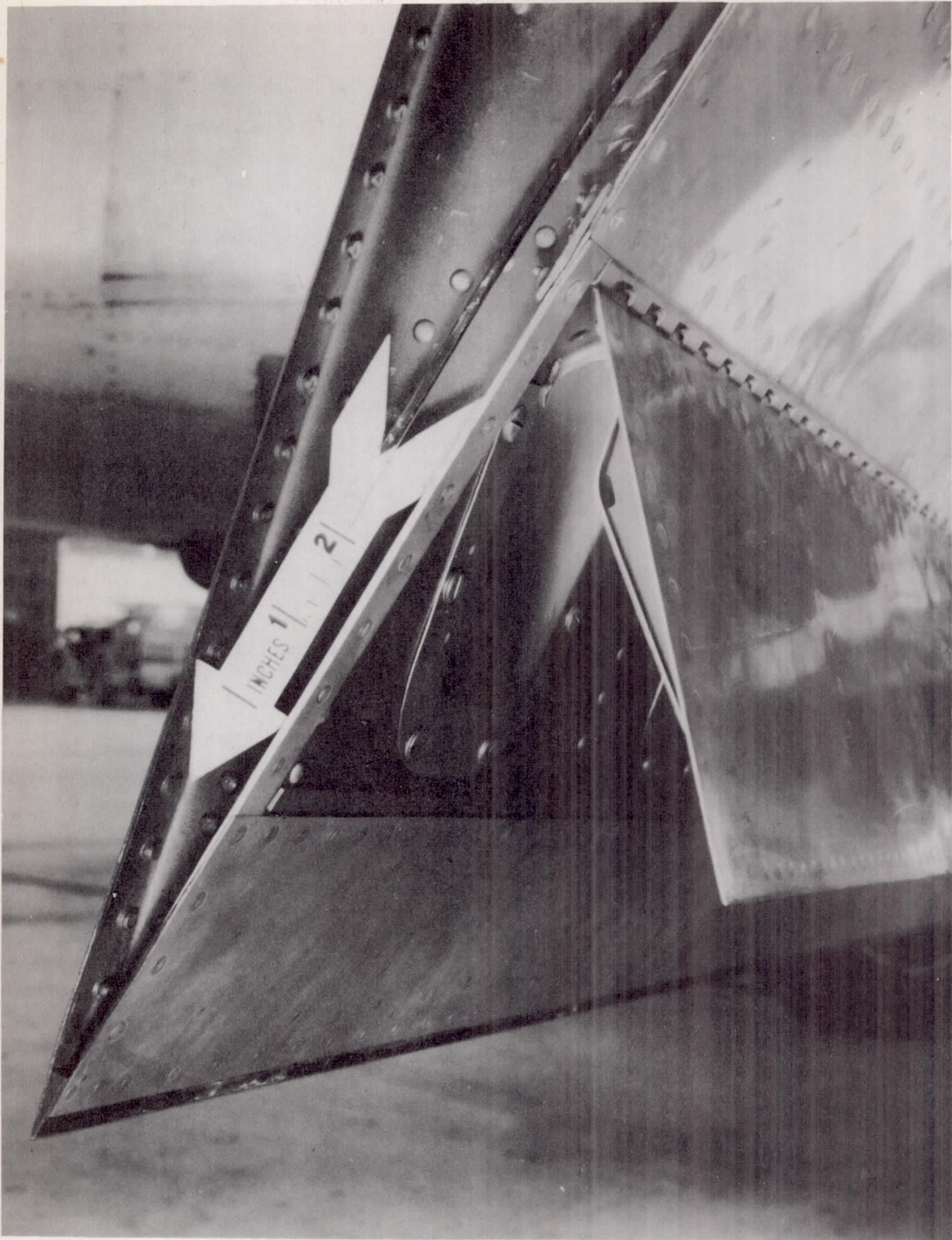


Figure 6.- View showing ducting at root of flap.

A-21688



A-21894

Figure 7.- Undersurface of flap showing split flap to cover ejector exits.

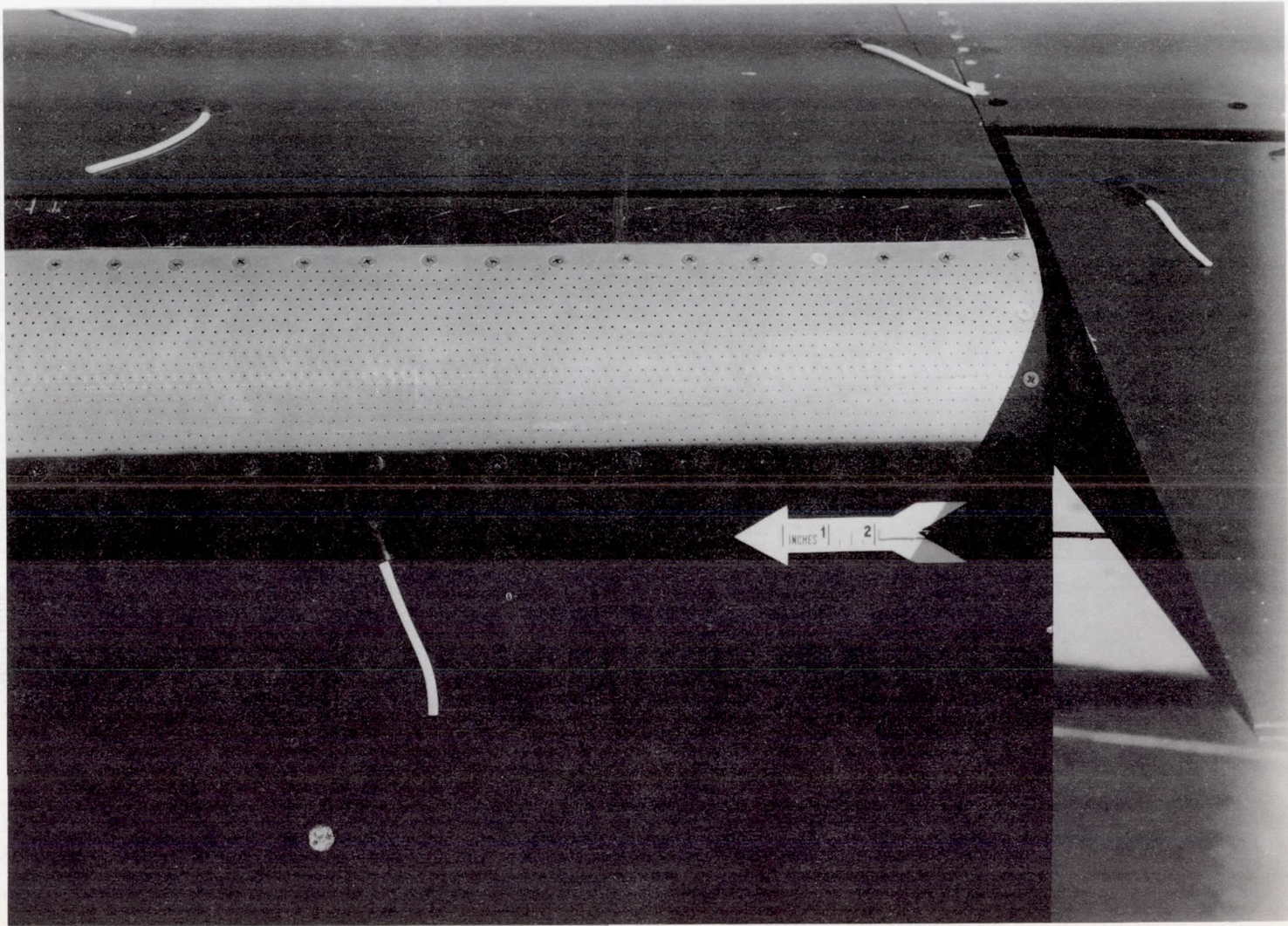
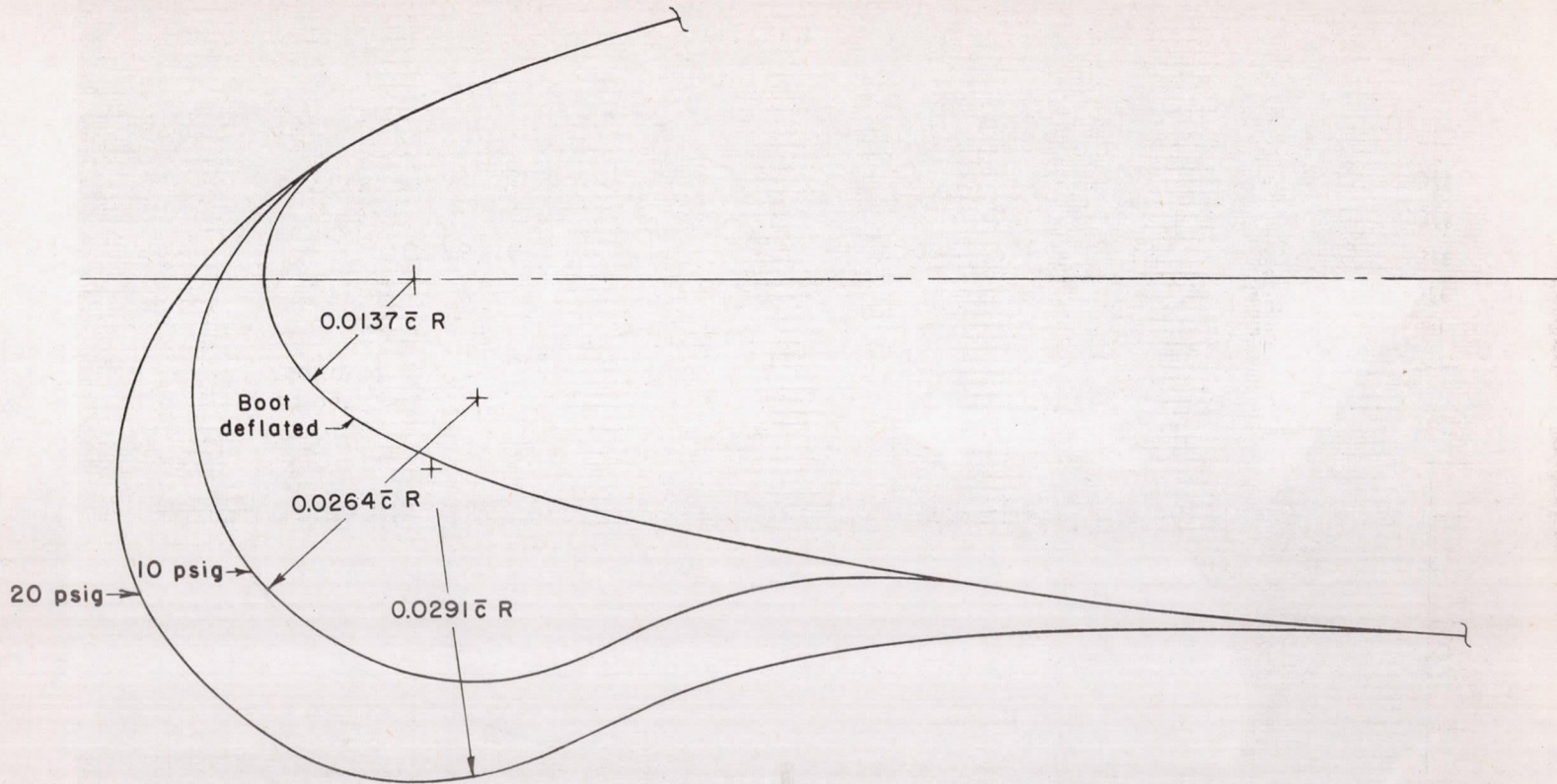


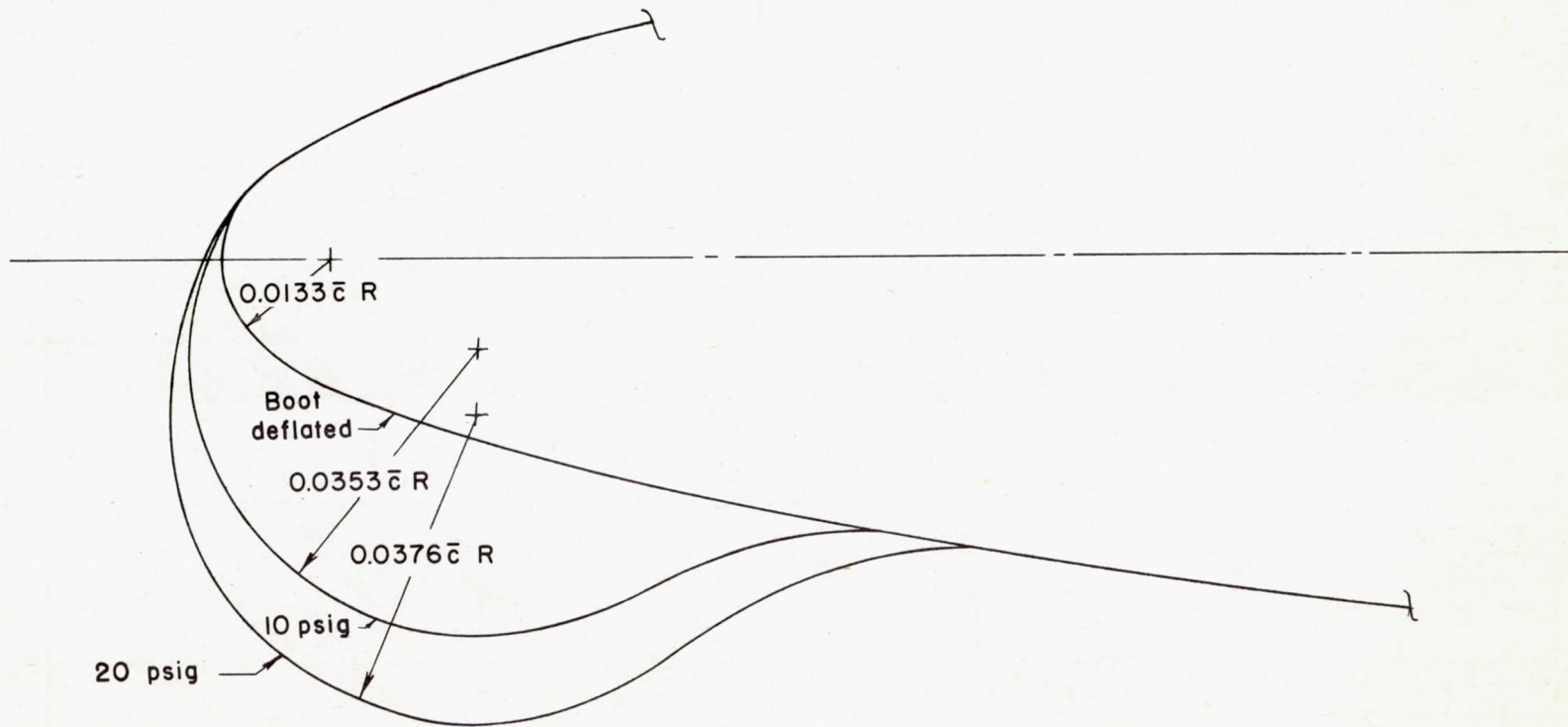
Figure 8.- Perforated 2024-T3 aluminum used on upper flap surface.

A-21892



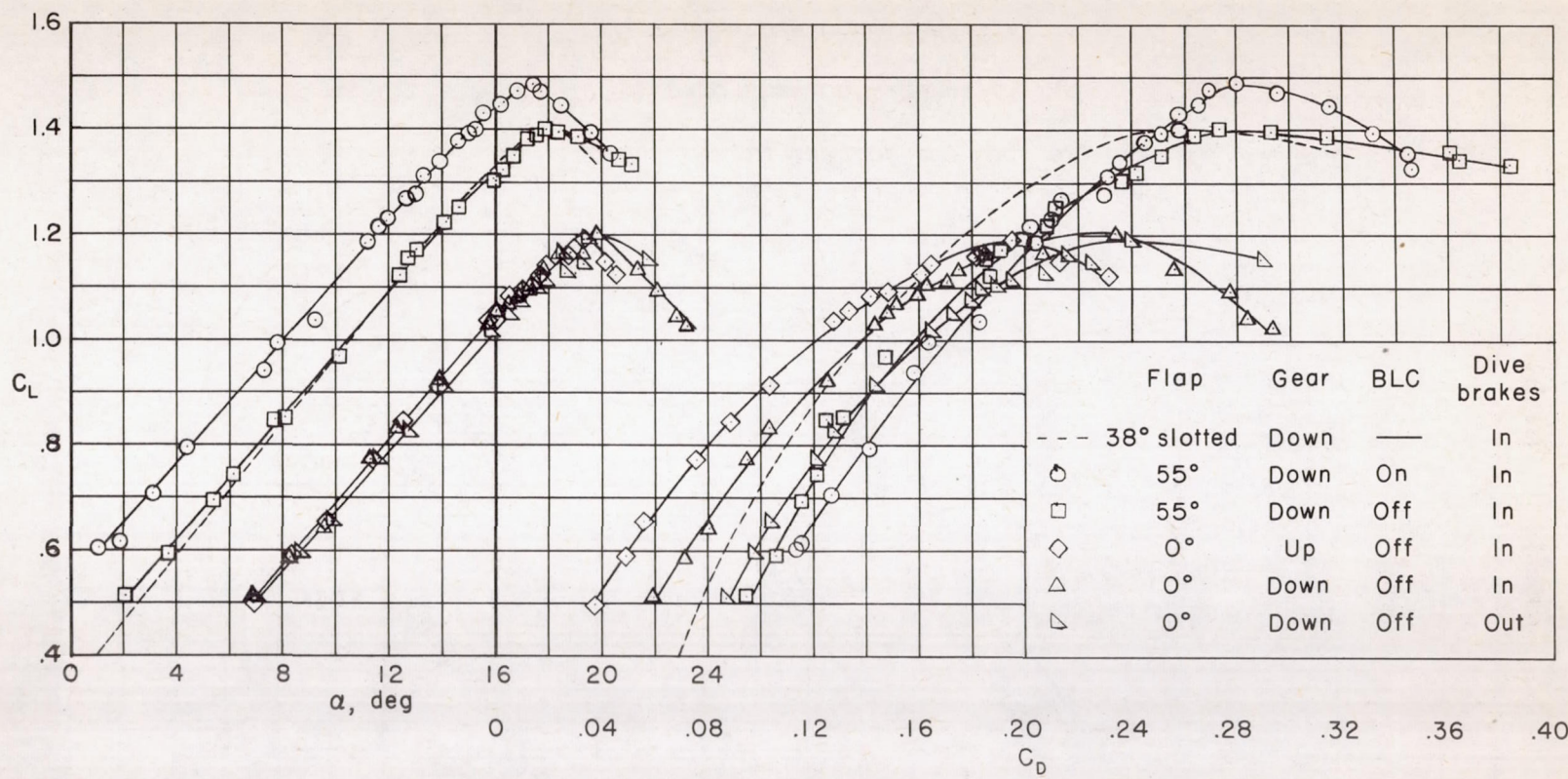
(a) Wing station  $0.165 b/2$ :

Figure 9.- Profile of airfoil taken perpendicular to wing leading edge with inflatable rubber boot; boot extent,  $0.146 b/2$  to  $0.96 b/2$ .



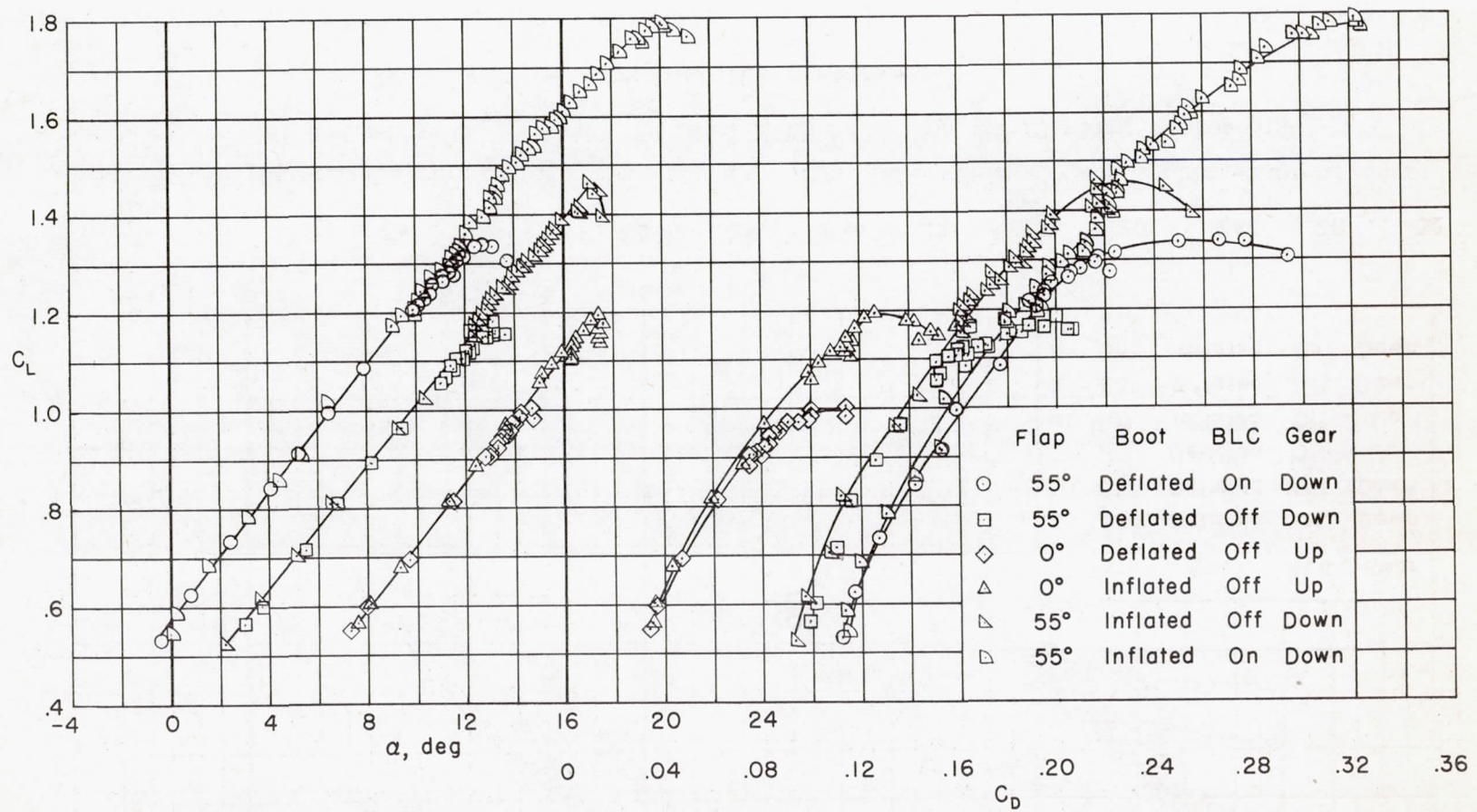
(b) Wing station 0.893 b/2.

Figure 9.- Concluded.



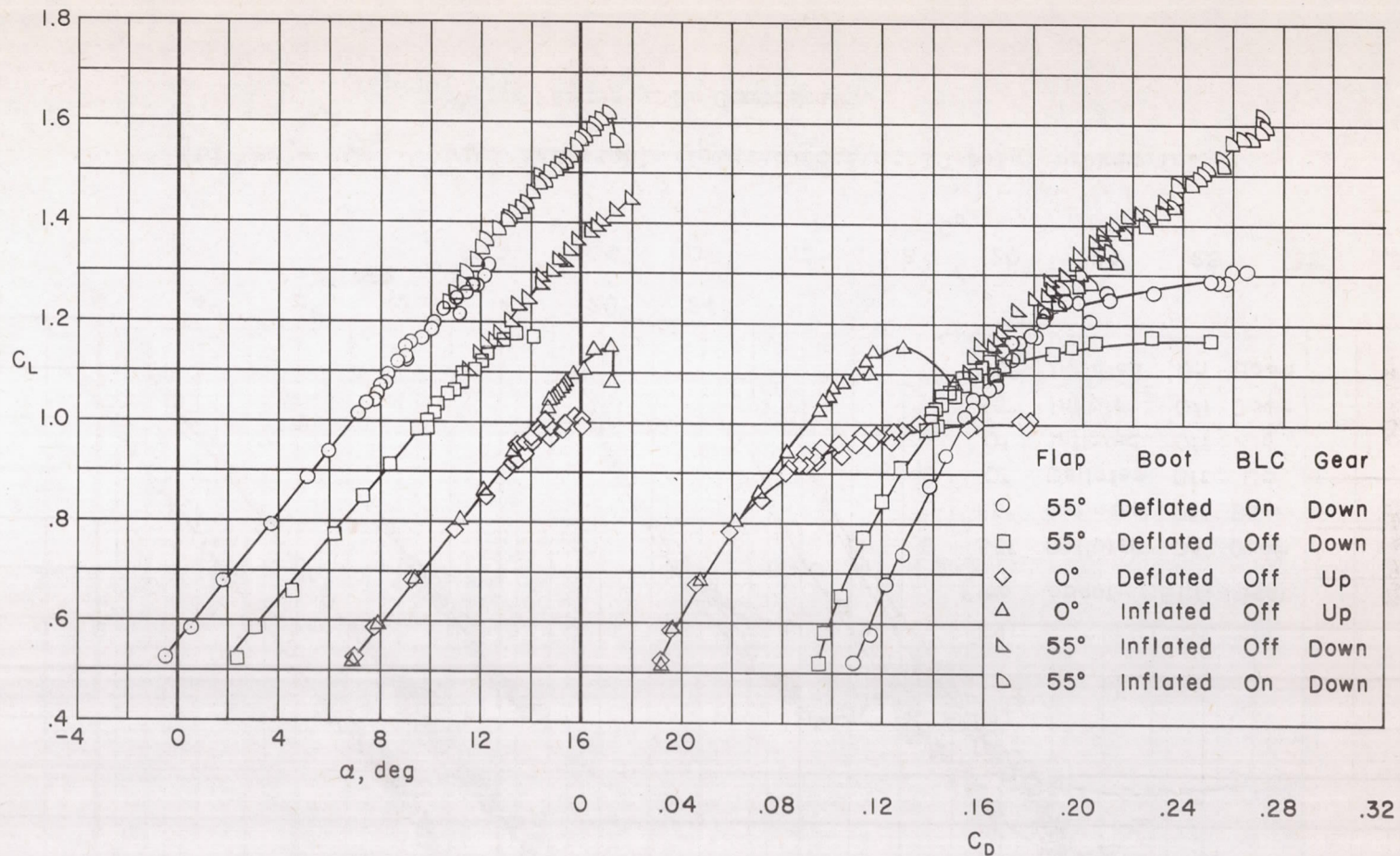
(a) Slatted leading edge.

Figure 10.- Lift and drag curves for 55° flap deflection and various wing leading-edge devices; 80 percent engine rpm.



(b) Large  $C_{L_{max}}$  with inflatable leading edge at 10 psig; brakes in.

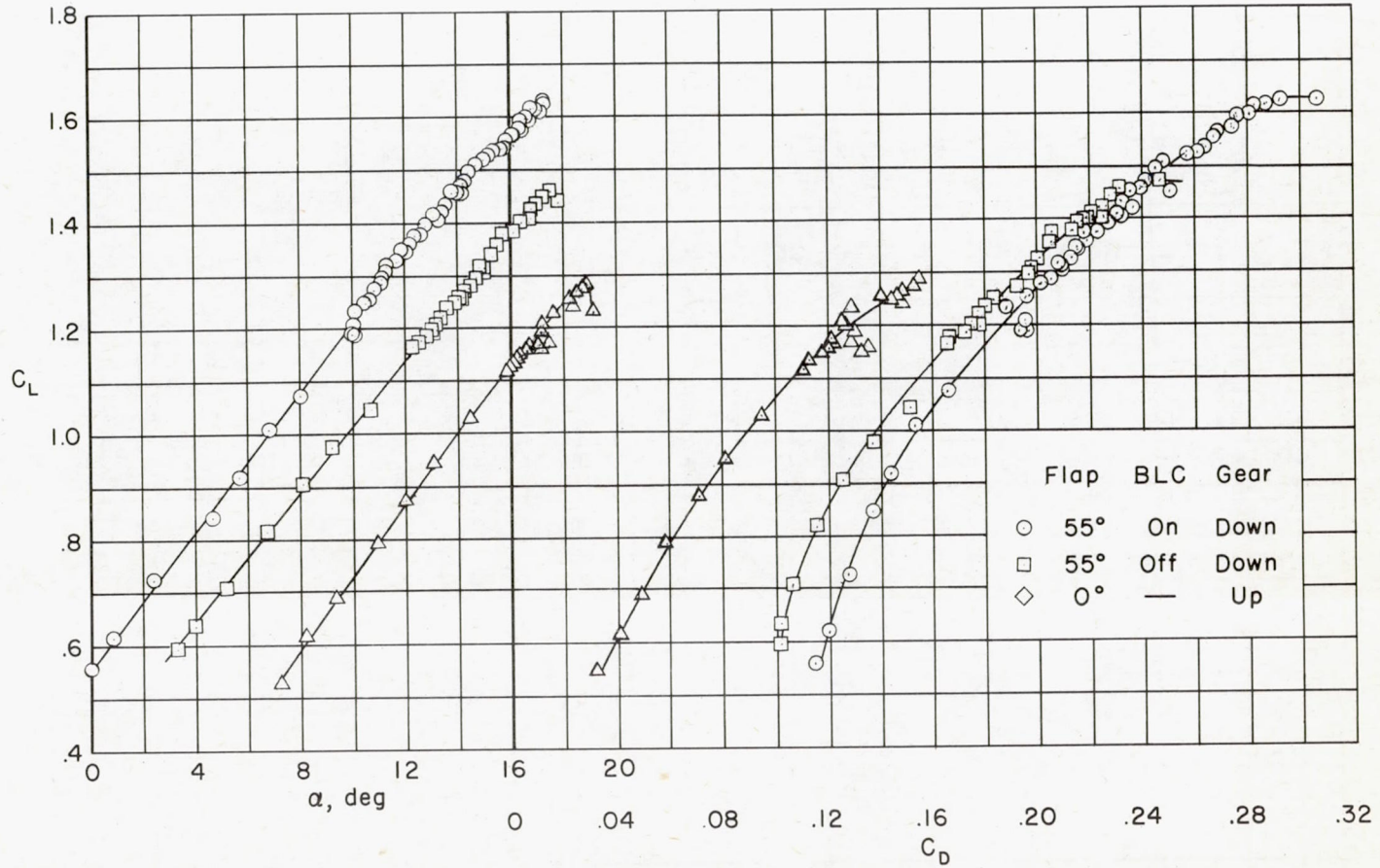
Figure 10.- Continued.



(c) Moderate  $C_{L_{max}}$  with inflatable leading edge at 10 psig; brakes in.

Figure 10.- Continued.





(d) Moderate  $C_{L_{max}}$  with leading edge inflated to 20 psig; brakes in.

Figure 10.- Concluded.

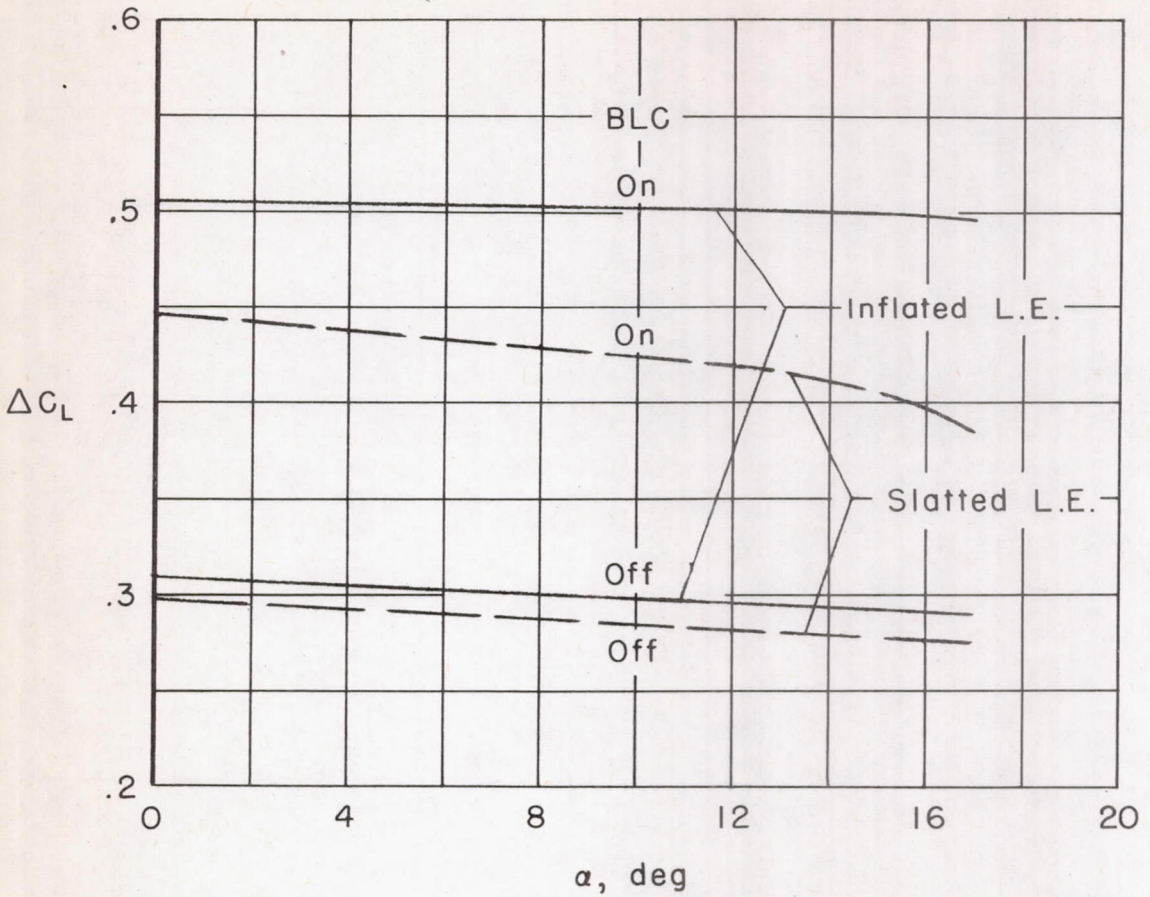


Figure 11.- Effect of leading-edge configuration on flap lift increment;  $\delta_f = 55^\circ$ , 80 percent engine rpm.

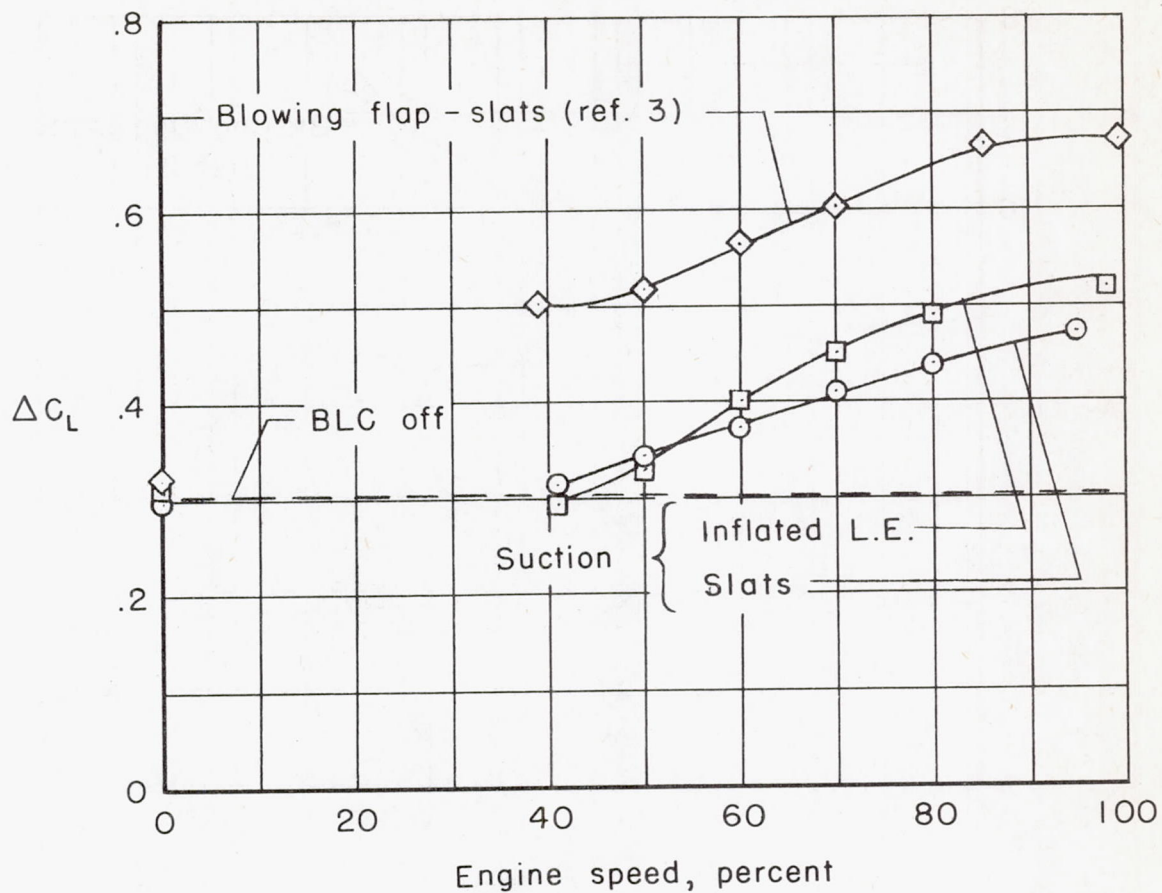


Figure 12.- Variation of flap lift increment with engine speed;  
 $\alpha = 11^\circ$ ,  $\delta_f = 55^\circ$ .

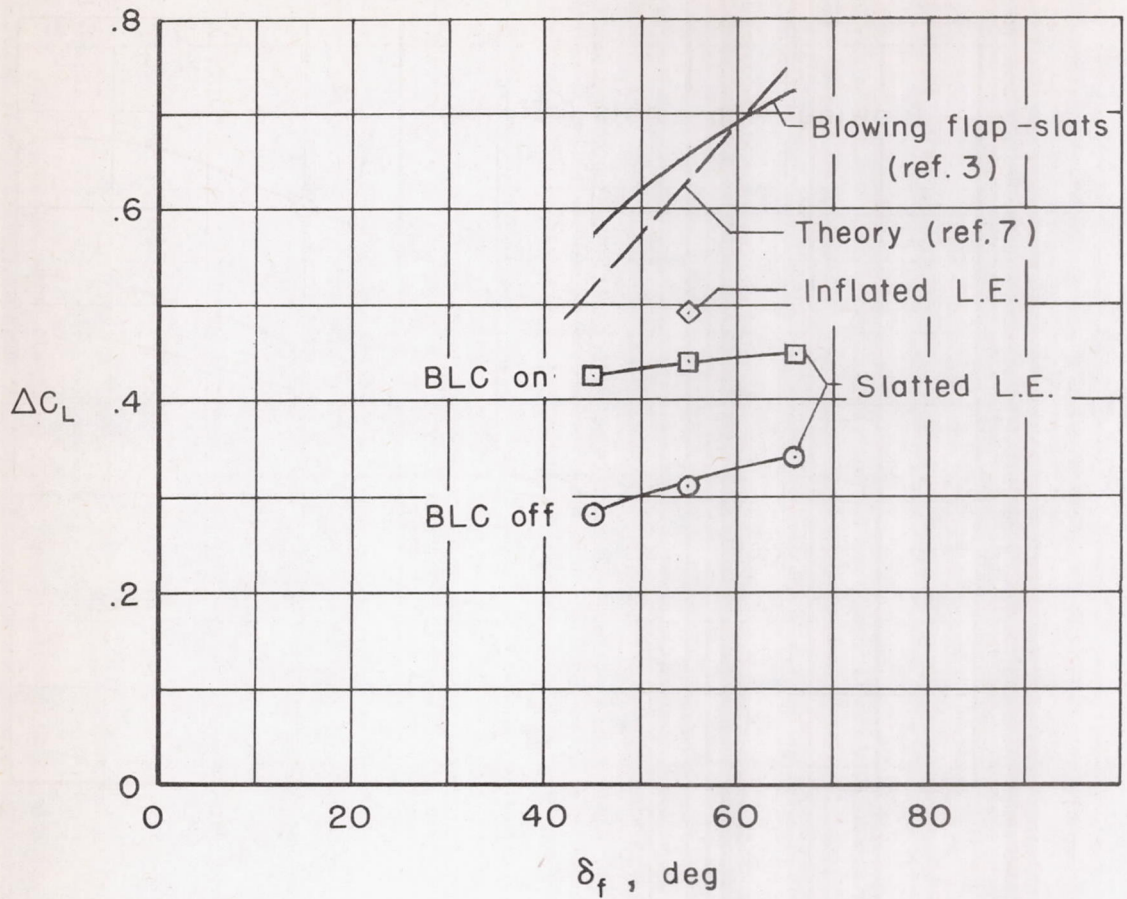


Figure 13.- Variation of flap lift increment with flap deflection; 80 percent engine rpm,  $\alpha = 8^\circ$ .

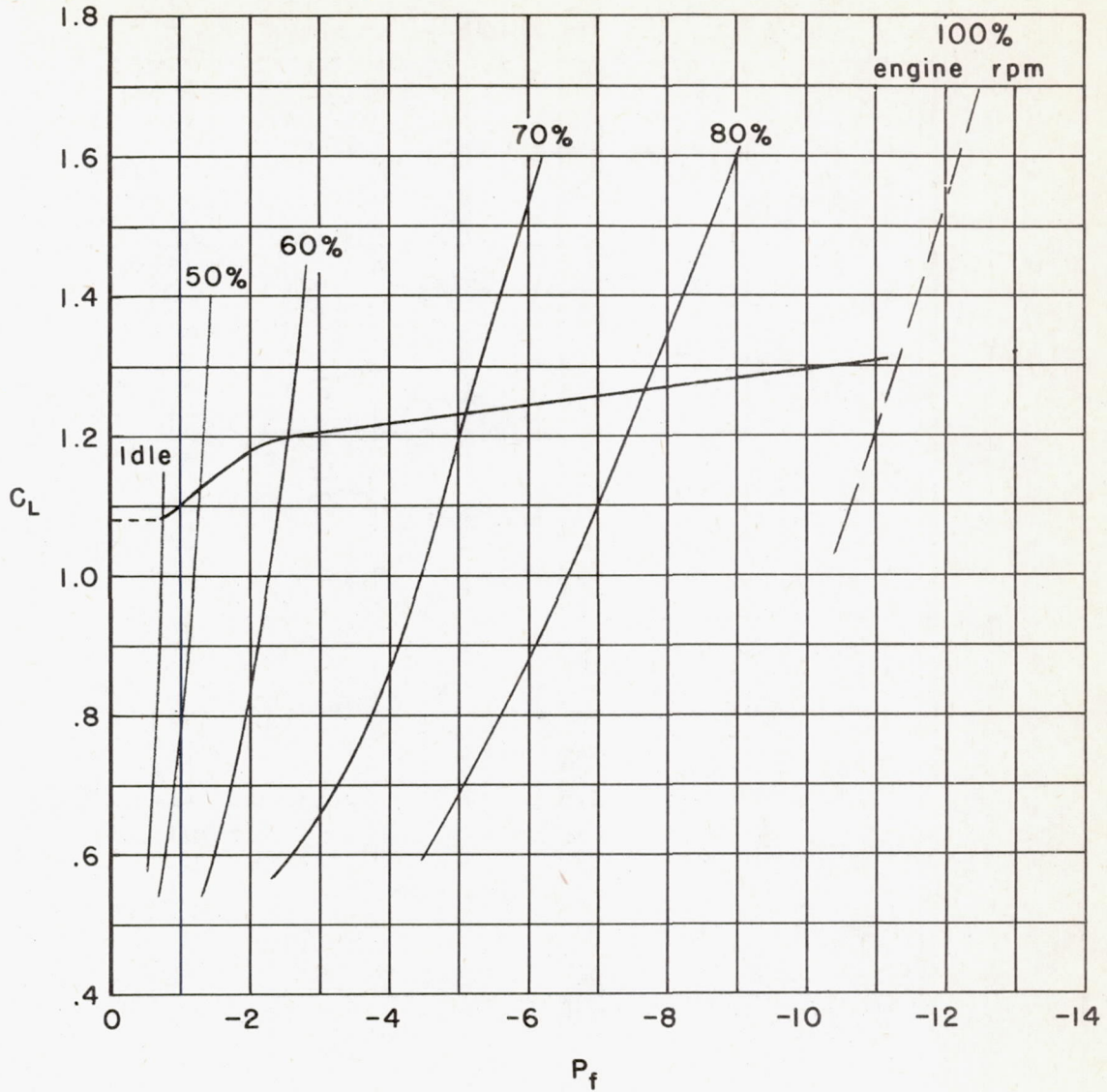


Figure 14.- Variation of airplane lift coefficient with duct pressure coefficient for  $\alpha = 11^\circ$  and various engine rpm.